Conférence Internationale en Automatique & Traitement de Signal (ATS-2018)
Proceedings of Engineering and Technology – PET
Vol.36 pp.29-34

Control of a photovoltaic pumping system

Z. Layate[#1], T. Bahi[*2], S. Lekhchine[¤3]

[#] *Department of technology, Djilali Bounaama University*
Khemis Miliana, Ain Defla,44001, Algeria
[1]zakarialayate@gmail.com

[*]*Second Company Automatic Laboratory and Signals LASA, Badji Mokhtar University*
Annaba, 23000, Algeria
[2]tbahi@hotmail.fr

[¤] *Departement of electrical engineering, 20 August 1955-Skikda University*
Skikda, 21000, Algeria
[3]slekhchine@yahoo.fr

***Abstract*— The encouragement shown in the development and proliferation of photovoltaic (PV) systems has allowed designers of power generation chains to invest in the field of renewable energies (RE). Systems used for converting solar energy into electricity are based on photovoltaic cells. Indeed, the association of modules consisting of series and parallel grouped cells forms a photovoltaic generator (GPV). However, the operation of the GPV depends essentially on the temperature (T) and the illumination (E), which have to lead to optimal operation, ie to extract the maximum produced power and thus to improve the installation performances whatever the climatic conditions, a maximum power point tracker (MPPT) control would be necessary. Then, due to the remarkable performances, the GPV have became the fundamental structure of pumping systems installed in isolated places.**

In this work, the performances of a water pumping system based on an asynchronous motor and a centrifugal pump, are analyzed under different climatic conditions.

***Keywords*— Renewable energy, PV system, pumping, MPPT, control.**

I. INTRODUCTION

The energy needs of industrialized societies are constantly increasing in order to meet the requirements of expected developments. Despite the existence of water probes, the inhabitants of the isolated sites remain to be deprived of drinking water and also irrigation because of the absence of electrification for reasons of accessibility, remoteness or others. However, by encouraging the development of renewable energy-based production systems, water pumping is then among the properties problems to be overcome in the most rural and Saharan regions. Indeed, the employment of photovoltaic solar (PV) energy-based water pumping is a well-adapted solution for these regions. Moreover, geographical situation of Algeria favours the development of the use of solar energy. These advantages could be beneficial in the remotest areas especially in water pumping applications. [1,2]. The PV water-pumping system consists of a PV generator, a power converter, a motor and pump. Ultimately, this system is economically justified where the energy supplied by the generator is stored in water pumped form during the day instead of being stored as electrical energy.

II. MODELLING OF THE PUMPING CHAIN

The pumping system is the combination of a set interconnected subsystems which are: the photovoltaic generator (GPV), the adapter chopper (DC / DC), 'MPPT' control, the voltage inverter, the induction cage motor and centrifugal pump[3-5]. The PV pumping chain is schematically shown in Fig.1.

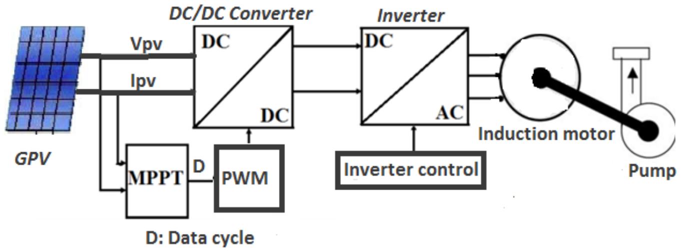

Fig. 1 synoptic diagram of photovoltaic pumping system

A. Photovoltaic generator

The equivalent circuit of photovoltaic cell is shown in Fig.2. The current I_{ph} is proportional to the incident illumination [6-8].

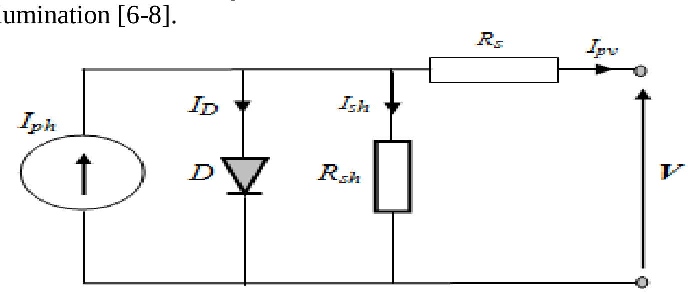

Fig. 2 PV cell equivalent circuit

By using the expression of diode current theory, the photovoltaic cell current can be expressed by the following formula:

ISSN 2356-5608

$$I_{pv} = I_{ph} - I_D - I_{sh} \quad (1)$$

The PV model can be established such as [9]:

$$I_{pv} = N_p I_{ph} - N_p I_0 \left(\exp\left(\frac{q\left(V_{pv} + \frac{N_s}{N_p} R_s I_{pv}\right)}{n K T N_s}\right) - 1\right) - \frac{V_{pv} + \frac{N_s}{N_p} R_s I_{pv}}{\frac{N_s}{N_p} R_{sh}}$$

Where,

- I_0 : Saturation current (A)
- q : Electron charge (1.6 10-19 C)
- K : Boltzmann constant (1.38 10-23 J/K)
- n : Ideality factor
- T : Cell temperature
- N_p : Number of cells in parallel
- N_s : Number of cells in series

The most usually external PV cell characteristics are shown in Fig. 3, Fig. 4, Fig. 5 and Fig. 6, under different conditions.

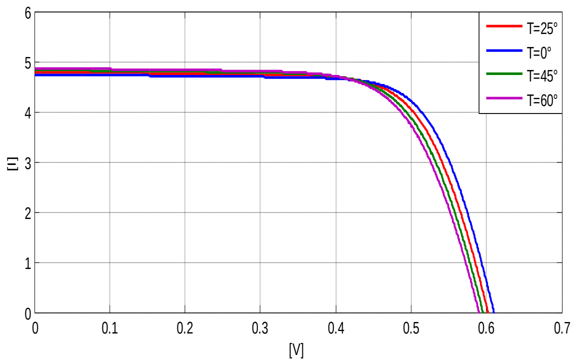

Fig. 3 I= f(V) of PV cell with G= 1000W/m2 and variable T

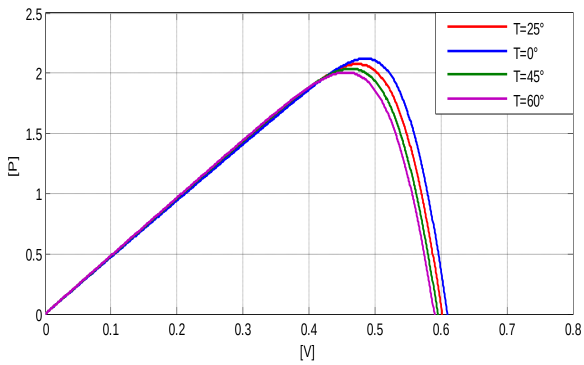

Fig. 4 P= f(V) of PV cell with G= 1000W/m2 and variable T

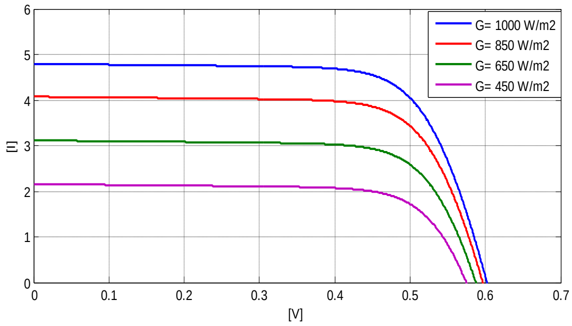

Fig. 5 I= f(V) of PV cell with T= 25°C and variable G

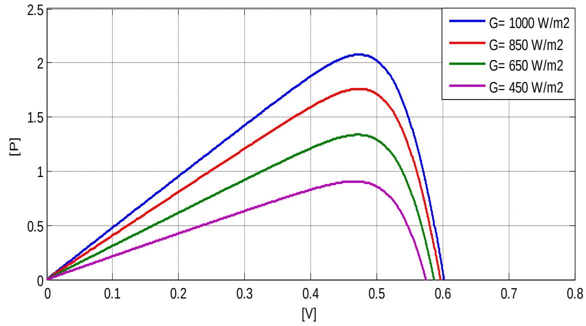

Fig. 6 P= f(V) of PV cell with T= 25°C and variable G

B. Model of the Boost converter

Boost converters are frequently used in photovoltaic applications, their DC output voltage is greater than its DC input contained voltage. Mainly, It consists of two (2) semiconductors switching components [10]. diode D and IGBT transistor T and two (2) parallel RC circuits at the input (Ri // Ci) and at the output (Ro // Co) as shown in Fig. 7.

The principle operating of the booster chopper is summarized in two distinct states: Firstly, When the transistor is in the closed state T_{on}, the current in the RL circuit increases and the energy is stored in the inductor. Then, when it is in the open state T_{off}, the current continues to cross the inductance through the diode D. Moreover, The switching period T_c and the variable duty ratio α are respectively defined by the following relationships:

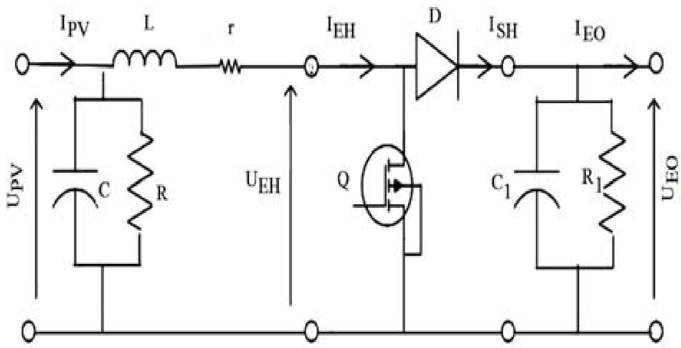

Fig.7 Boost converter

ISSN 2356-5608

$$T_c = T_{on} + T_{off} \tag{3}$$

$$\alpha = \frac{T_{on}}{T_{on} + T_{off}} \tag{4}$$

C. Maximum power point tracking control

Regardless climatic variations, The PV modules must be operated at their maximum Power point. Among the most widely used algorithms for tracking the peak power point are both the perturb and observe (P&O) and the incremental conductance (IC) [11-12]. In this work, we use the P & O method.

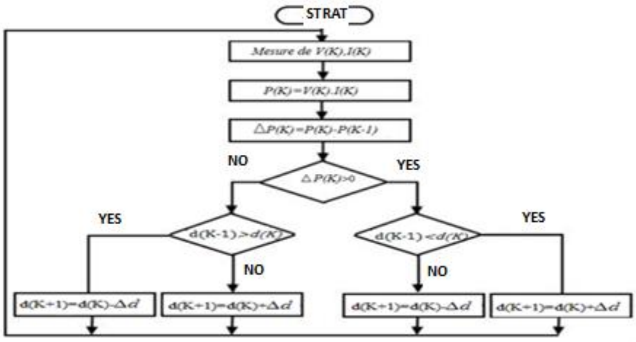

Fig. 8 P&O flowchart algorithm

D. Modelling and control of inverter

The three-phase inverter allows to an optimal power transfer between the set GPV-pump whatever the conditions of produced power and power demand. In this work, a PWM inverter is used to control the motor speed. Thus, the controller sends pulses (S1 to S6) to the gates of PWM inverter in which the actual motor speed (N) tracks the reference speed (Nref) set by the dc-link voltage controller.

$$\begin{bmatrix} V_{an} \\ V_{bn} \\ V_{cn} \end{bmatrix} = \frac{V_{dc}}{3} \begin{bmatrix} 2 & -1 & -1 \\ -1 & 2 & -1 \\ -1 & -1 & 2 \end{bmatrix} \begin{bmatrix} S_1 \\ S_2 \\ S_3 \end{bmatrix} \tag{5}$$

With,

Vin (i=1, 2 and 3) are the output voltages ;
Vdc : input voltage of inverter ;
Si =0 or 1 for i=1, 2, and 3 are the PWM control signals.

E. Motor Modelling

The equipping motor pump machine of the studied system is an induction type. The mathematical model of an induction motor (IM) can be established using d-q transformation as described by the following equation system:

$$\begin{cases} V_{ds} = R_s i_{ds} + \dfrac{d\phi_{ds}}{dt} - \omega_s \phi_{qs} \\ V_{qs} = R_s i_{qs} + \dfrac{d\phi_{qs}}{dt} + \omega_s \phi_{ds} \\ V_{dr} = 0 = R_r i_{dr} + \dfrac{d\phi_{dr}}{dt} + \omega_r \phi_{qr} \\ V_{qr} = 0 = R_r i_{qs} + \dfrac{d\phi_{qs}}{dt} - \omega_r \phi_{dr} \end{cases} \tag{6}$$

$$\begin{cases} \phi_{ds} = L_s i_{ds} + M i_{dr} \\ \phi_{qs} = L_s i_{qs} + M i_{qr} \\ \phi_{dr} = L_r i_{dr} + M i_{qr} \\ \phi_{qs} = L_r i_{qr} + M i_{qs} \end{cases} \tag{7}$$

With;

$$\omega_s = p\Omega = \omega_s - \omega_r \tag{8}$$

The latter can be derived from the equation of co-energy or deduced from the power budget.

$$T_e = \frac{pM}{Lr} (\Phi_{dr} i_{sq} - \Phi_{qr} i_{ds}) \tag{9}$$

$$Te - Tl = J\frac{d\Omega}{dt} + k_f \Omega \tag{10}$$

With;

Rs	stator motor resistance
Rr	rotor motor resistance
Ids, Iqs :	d-q stator currents
ϕds, ϕqs :	d-q stator flux
Vds, Vqs :	d-q stator voltages
Idr, Iqr :	d-q rotor currents
ϕdr, ϕqr :	d-q rotor flux
ω_s :	stator electrical pulsation
ω_r :	rotor electrical pulsation
Ls :	stator inductance
Lr :	rotor inductance
Lm :	motor mutual inductance
P :	motor pole pairs number
Te :	motor torque
Tr :	load torque

ISSN 2356-5608

f : friction coefficient
J : total inertia
Ω : mechanical speed

F. Vector control strategy of the induction motor

In case of centrifugal pump, assuming that DC/DC and DC/AC converters are ideal, the PM output power of the GPV is given by the following equation [13,14]:

$$PM = \frac{C_1(1-S)^3}{\eta} f^3 \tag{11}$$

with ,

C1 : constant..
η: motor pump yield (%).
f : Inverter output voltage frequency (Hz).
S : slip.

In the standard conditions, *PM*, *η*, *f and S* become respectively: optimal power (PM_n), optimal efficiency ($\eta_0 = 0.6$) , the nominal frequency (f_n = 50 Hz) and optimal slip ($S_0 = 0.02$).

After analysis by introducing the above parameters in equation and making the ratio between *PM* and PM_n, the inverter control frequency is given by:

$$f = \sqrt[3]{\frac{PM}{PM_n}} f_n \tag{12}$$

Therefore, applying the vector control by orienting the rotor flux to the induction motor: The direct rotor flux $\phi_{rd} = \phi_r$ and the quadratic rotor flux $\phi_{rq} = 0$.The expression of the electromagnetic torque is given by:

$$C_{em} = \frac{pM}{L}\phi_r i_{sq} \tag{13}$$

The expression of the rotor flux (*Eq*.14) is given as a function of the direct stator current (i_{sd}), maximum mutual inductance between a stator phase and a rotor phase (*M*) and time constant T_r :

$$\phi_r = \frac{M}{1+T_r} i_{sd} \tag{14}$$

The rotor speed is estimated by the following equation:

$$\omega_r = \frac{M}{T_r \phi_r} i_{sd} \tag{15}$$

Then, the speed ω_s is given by the equation (Eq.16):

$$\omega_s = \frac{M}{T_r \phi_r} i_{ds} + p\Omega \tag{16}$$

The expression of the reference velocity is given by the following equation:

$$\Omega_{ref} = \sqrt[3]{\frac{Ppv}{k}} \tag{17}$$

G. Centrifugal pump model

The centrifugal pump applies a proportional load torque to the square of the speed :

$$T_l = K_{ch} \times \omega^2 \tag{18}$$

with, K_{ch} is a constant and ω is motor speed.

Knowing the performances of a centrifugal pump (Q, H and P) for the speed *N* , the laws of similarity make it possible to determine the performances (*Q*', *H*' et *P*') for *N*' using the following relationships [14,15]:

$$\begin{cases} Q' = \frac{N'}{N} Q \\ H' = H\left(\frac{N'}{N}\right)^2 \\ P' = P\left(\frac{N'}{N}\right)^3 \end{cases} \tag{19}$$

where, *Q* et *Q*' , the flow rates corresponding, respectively, to the speed N and N' , *H* and *H'* , the total anometric heights corresponding respectively to the speed *N* et *N*' , *P* et *P'* are the power motor the powers of the motor respectively corresponding to the speed *N* and *N*'.

The *H (Q)* characteristic of centrifugal pump is obtained using Pleider-Peterman model [16,17]. The multispeed can be expressed approximately by the following quadratic form:

$$H = C_1\omega^2 - C_2\omega Q - C_3 Q^3 \tag{20}$$

The pipe resistance characteristic can be given by:

$$H = H_s + K_{fr} Q^2 \tag{21}$$

ISSN 2356-5608

Conférence Internationale en Automatique & Traitement de Signal (ATS-2018)
Proceedings of Engineering and Technology – PET
Vol.36 pp.29-34

The hydraulic power of the pump is given by:

$$Ph = \rho.g.Q..H \tag{22}$$

With;

C_1, C_2, C_3 :	coefficients given by the manufacturer.
H_s :	pump static head.
K_{fr} :	canalization constant.
K_{ch} :	Proportionality constant.

III. Simulation Results and Discussion

The developed simulink program was tested under temperature and illumination conditions and according to their evolutions shown, respectively, by Figures 9 and 10. FIG. 11 represents the DC voltage at the output of the photovoltaic panel and that of Fig. 12 shows a Zoom on the voltage at the output of the inverter. Finally, the flow rate of the pump is shown given, for the preceding conditions in FIG. 13.

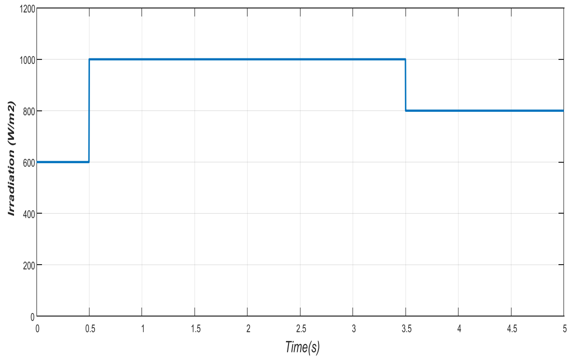

Fig.9 illumination profile

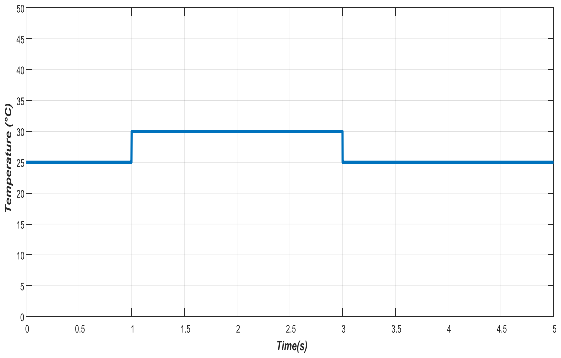

Fig.10 Temperature variation

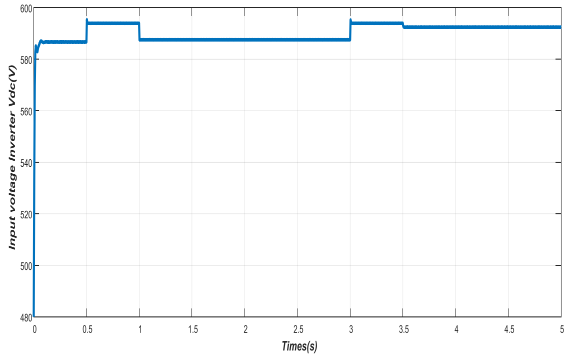

Fig.11 Input voltage inverter (*Vdc*)

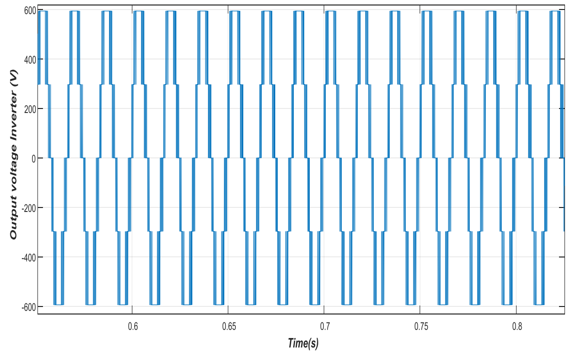

Fig.12 Zoom on output voltage inverter (V)

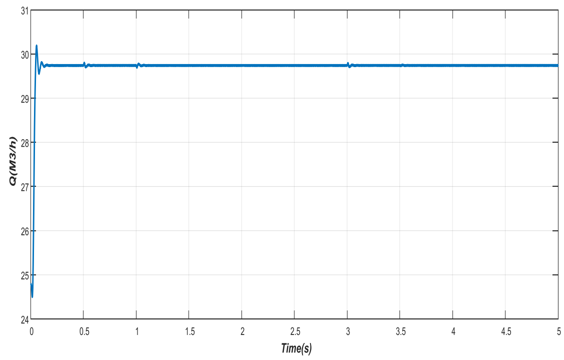

Fig.13 Flow of the pump

IV. Conclusions

In this work, a motor pump powered by a photovoltaic generator via a three-phase voltage inverter is studied. For this purpose, performances are analysed under weather changes. The perturb and observe algorithm is used to extract the maximum power. The simulation results of the photovoltaic chain and the pumping stations are represented.

ISSN 2356-5608

REFERENCES

[1] S. Boukebbous, D. Kerdoun, International ournal of Renewalable Energy Research, , Vol.7, No.4, 2017.

[2] W. Cai, H. Ren, Y. Jiao, M. Cai, X. Cheng, " Analysis and simulation for grid-connected photovoltaic system based on Matlab",*IEEE, International conference on electrical and control enginnering, ICECE,* pp.63-66, september 2011.

[3] K. Himour, K. Ghedamsi, E.M. Berkouk, "A five-level diode clamped inverter for grid connection PV generation system", *International renewable and sustainble energy conference, IRSEC'2013*, ouarzazate, March 07-09, 2013.

[4] Y. Liu, B. Ge, H. Abu-rab, F. Z. Peng, " Control system design of battery-assisted quazi-Z-source inberter for grid-tie photovoltaique power generation", *IEEE ,Transaction on sustainable energy*, Vol. 4, N°. 4, pp. 994-1001, october 2013.

[5] R. F. Coelho, L. Schimtz, D. C. Martins, " Grid-connected PV-Wind-Fuel cell hybrid system employing supercapacitor bank as storage device to supply a critical DC load", *IEEE, 33rd international telecommunications energy conference, INTELEC*, 2011.

[6-11] CN. Bhende ,SG Malla, Novel control of photovoltaic based water pumping system without energy storage. Int JEmerg Electric Power Syst , 13(5), 2012.

[7-17] R. Krishnan, Electric motor drives: modeling, analysis andcontrol. Upper Saddle River, NJ: Prentice-Hall; 2001.

[8- 18] J. Lepka, P. Stekl, 3-Phase AC induction motor vector control using a 56F80x, 56F8100or56F8300 device. Free scale semiconductor,applicationnote,AN1930, Rev.2;2/2005.

[9-19] GR. Whitfield ,et al, Increasing the cost effectiveness of small solar photo- voltaic pumping systems. Renew Energy ,September, 1995.

[10] A. Meflah , T. Allaoui, Commande d'une chaîne de pompage photovoltaïque au fil du soleil, Revue des Energies Renouvelables Vol. 15 N°3 , p. 489 – 499, 2012.

[11] A. Henchiri , T. Bahi, L. Khochemane, Performances of solar photovoltaic under different climatic conditions , CIMSI, November 2017, Mecanical Deparment, Skikda University, Algeria.

[12] N. Priyadarshi, A. Anand, A. Sharma, F. Azam, V. Singh, R. Sinha, "An Experimental Implementation and Testing of GA based Maximum Power Point Tracking for PV System under Varying Ambient Conditions Using dSPACE DS 1104 Controller", International Journal of renewable energy research , IJRER, Vol.7, N°1, pp.255-265, 2017.

[13] M.F. Mimouni, M.N. Mansouri, B. Benganem and M. Annabi, 'Vectorial Command of an Asynchronous Motor Fed by a Photovoltaic Generator', Renewable Energy, Vol. 29, N°3, pp. 433 – 442, 2004.

[14] Ghosh A, et al. Small-signal modelling and control of photovoltaic based water pumping system. ISA Transactions (2015), http://dx.doi.org/10.1016/j.isatra.2015.01.008i.

[15] Hamad Raad Salih, Ali Abdulwahhab Abdulrazzaq,Basarab Dan Guzun, Dynamic Modeling of Pump Drive System utilizing Simulink/MATLAB Program, International Research Journal of Engineering and Technology (IRJET) , Vol. 03 , N° 01, p.21 :24. Jan-2016.

[16] L. Elmahni, L. Bouhouch and A. Moudden, Smart management of a photovoltaic pumping station located in the Agadir region, International Journal of Innovation and Applied Studies, ISSN 2028-9324 Vol. 18 No. 4, pp. 1216-1227, Dec. 2016.

[17] N. Johnson, S.A. Kannan, G. Paul, J. Jose, J. George, " Modeling of solar power based Quasi-Z-Source inverter to Supply BLDC Motor", International journal of innovative research in electrical, electronics, instrumentation and control engineering, Vol. 2, Issue 2, February 2014.

ISSN 2356-5608